

PSI

F  
FONDAZIONE  
BRUNO KESSLER

# Characterization of charge integrating detectors with iLGAD sensors in the soft X-ray energy range

M.<sup>o</sup>Carulla<sup>1</sup>, R.<sup>o</sup>Barten<sup>1</sup>, F.<sup>o</sup>Baruffaldi<sup>1</sup>, A.<sup>o</sup>Bergamaschi<sup>1</sup>, A.<sup>o</sup>Bisht<sup>2</sup>, M.<sup>o</sup>Boscardin<sup>2</sup>, B.<sup>o</sup>Braham<sup>1</sup>, M.<sup>o</sup>Brückner<sup>1</sup>, M.<sup>o</sup>Centis Vignali<sup>2</sup>, R.<sup>o</sup>Dinapoli<sup>1</sup>, S.<sup>o</sup>Ebner<sup>1</sup>, K.<sup>o</sup>Ferjaoui<sup>1</sup>, F.<sup>o</sup>Ficarella<sup>2</sup>, E.<sup>o</sup>Fröjd<sup>1</sup>, D.<sup>o</sup>Greffenberg<sup>1</sup>, O.<sup>o</sup>Hammad<sup>o</sup>Ali<sup>2</sup>, S.<sup>o</sup>Hasanaj<sup>1</sup>, J.<sup>o</sup>Heymes<sup>1</sup>, V.<sup>o</sup>Hinger<sup>1</sup>, T.<sup>o</sup>King<sup>1</sup>, P.<sup>o</sup>Kozlowski<sup>1</sup>, C.<sup>o</sup>Lopez-Cuenca<sup>1</sup>, D.<sup>o</sup>Mezza<sup>1</sup>, K.<sup>o</sup>Moustakas<sup>1</sup>, A. Mozzanica<sup>1</sup>, G.<sup>o</sup>Paternoster<sup>2</sup>, K.A. Paton<sup>1</sup>, S.<sup>o</sup>Rochin<sup>2</sup>, C.<sup>o</sup>Ruder<sup>1</sup>, B.<sup>o</sup>Schmitt<sup>1</sup>, P.<sup>o</sup>Sieberer<sup>1</sup>, D.<sup>o</sup>Thattil<sup>1</sup>, X.<sup>o</sup>Xie<sup>1</sup>, and J.<sup>o</sup>Zhang<sup>1</sup>

<sup>1</sup> Paul Scherrer Institut, Forschungsstrasse 111, 5232 Villigen-PSI, Switzerland

<sup>2</sup> Fondazione Bruno Kessler, Via Sommarive 18, 38126 Povo TN, Italy

[maria.carulla@psi.ch](mailto:maria.carulla@psi.ch)

25<sup>th</sup> iWoRID, Lisboa, July 2, 2024



Hybrid pixel detectors for photon science

2D detectors for soft X-rays

Challenges for soft X-rays detection

Development Strategy

QE improvement

iLGADs for soft X-ray detection

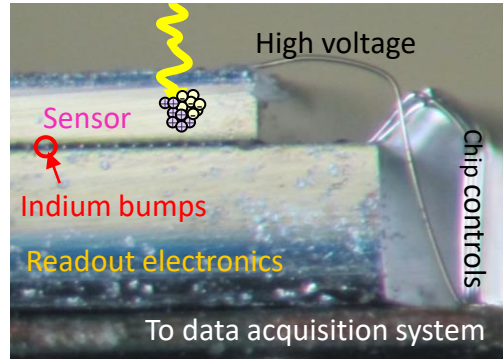
Depth dependence of gain in iLGADs

Single photon resolution

Comparison between gain layers



# Hybrid pixel detectors for photon science



- 😊 Sensor and readout are optimised separately
- 😊 Direct conversion
- 😊 Highly parallelised readout -> High frame rate(> 2kHz)
- 😊 Large area ( $> 4 \times 8 \text{ cm}^2$ ) tileable
- 😢 Bump bonding limits pixel pitch
- 😢 Input capacitance increases the electronic noise

## Single photon counting for synchrotrons



- 😊 Counts
- 😊 Fluorescence rejection



SLS 2.0 →

## Charge integrating for XFEL



- 😊 Large dynamic range
- 😊 High flux
- 😢 Calibration

Single photon resolution for soft X-rays

# 2D detectors for soft X-rays (200 eV to 2 keV)

## L-edges of 3d transition metals

- Mn, Fe, Cu, ...

## K-edges light elements and ‘water window’

- C, N, O, S, ...

RIXS & TR-RIXS



V. Hinger's talk, July 4 at 12:20

## Detector requirements:

- High QE for soft X-rays
- Large area
- Good spatial resolution ( $\sim 5 \mu\text{m}$ )

- Low noise (< 5 e- r.m.s)
- High frame rate (> 100 Hz SwissFEL)

## EMCCD

- 😊 High QE (55% @ 250 eV)
- 😢 Limited area ( $\sim 2 \times 2 \text{ cm}^2$ )
- 😊 High spatial resolution ( $\leq 5 \mu\text{m}$ )
- 😊 Low noise ( $\leq 1 \text{ e}^-$ )
- 😢 Slow readout ( $\sim 1 \text{ Hz}$ )

## Scientific CMOS

- 😊 High QE (62% @ 250 eV)
- 😢 Limited area ( $\sim 2 \times 2 \text{ cm}^2$ )
- 😢 High spatial resolution ( $\leq 10 \mu\text{m}$ )
- 😊 Low noise ( $\sim 1-2 \text{ e}^-$ )
- 😢 Frame rate (< 50 Hz)

## Hybrid pixel detectors

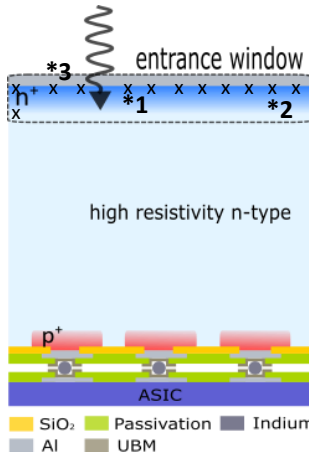
- 😢 Low QE (< 1 % @ 250 eV)
- 😊 Large area ( $> 4 \times 8 \text{ cm}^2$ ) tiled
- 😢 Spatial resolution ( $< 5 \mu\text{m}^*$ )
- 😢 Noise ( $\sim 35 \text{ e}^-$ )
- 😊 High frame rate(> 2kHz)

\*Interpolation with Mönch (Hard X-rays)

# Challenges for soft X-ray detection

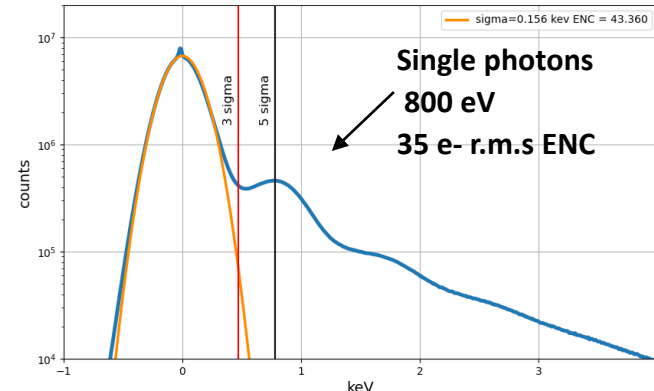
Low quantum efficiency

1. Auger recombination in n+  $L_h = 200\text{nm}$   
Conc  $\sim 10^{20} \text{ cm}^{-3}$
2. SRH recombination at Si/Al interface  
(  $S_0 \sim 10^7 - \infty \text{ cm/s}$  )
3. Absorption in the surface layers



Low signal-to-noise ratio

- o SNR  $\approx 1.6$  for 200 eV
- o SNR  $> 5$  is required to achieve single photon resolution



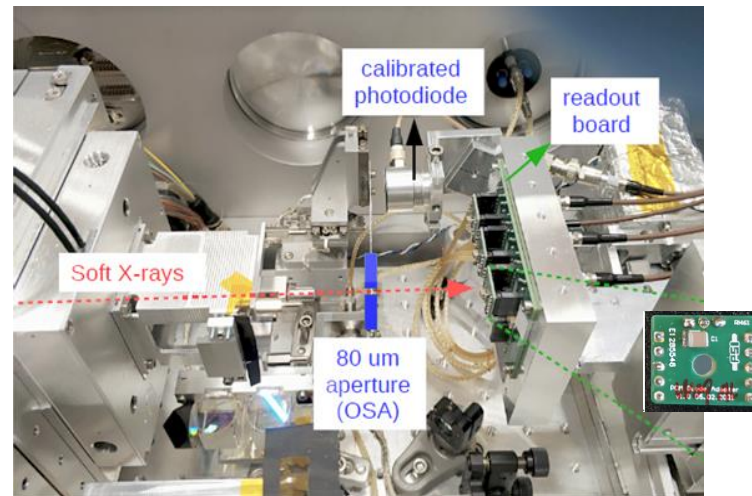
Reduce losses in the entrance window  
Entrance window technology

+ Increase the signal by internal multiplication  
iLGAD technology

V. Hinger et al 2022 JINST **17** C09027  
<https://doi.org/10.1088/1748-0221/17/09/C09027>

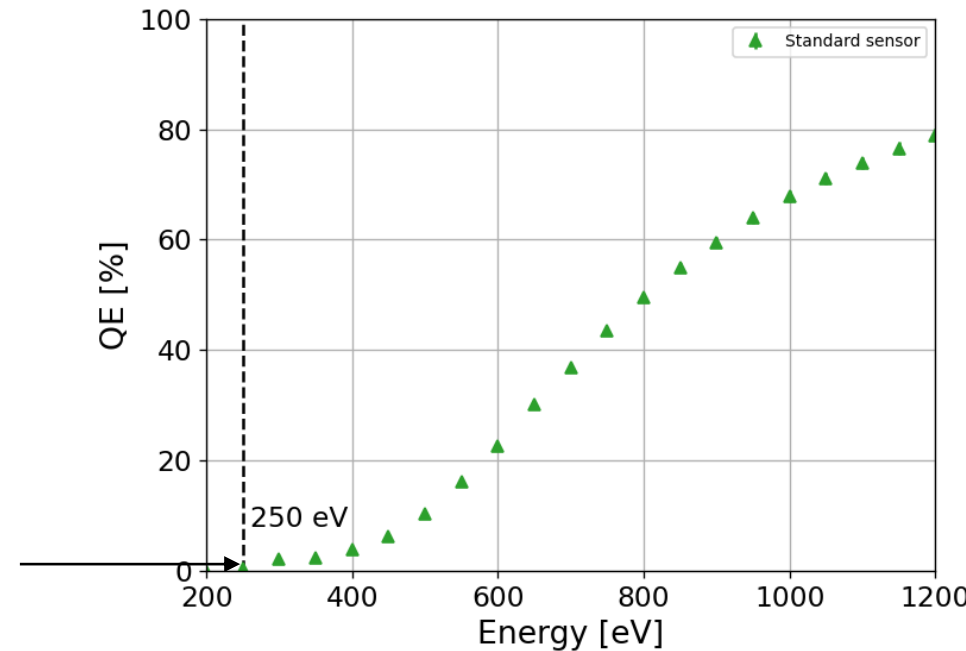
# QE improvement

## Setup at the Surface/Interfaces Microscopy (SLS)



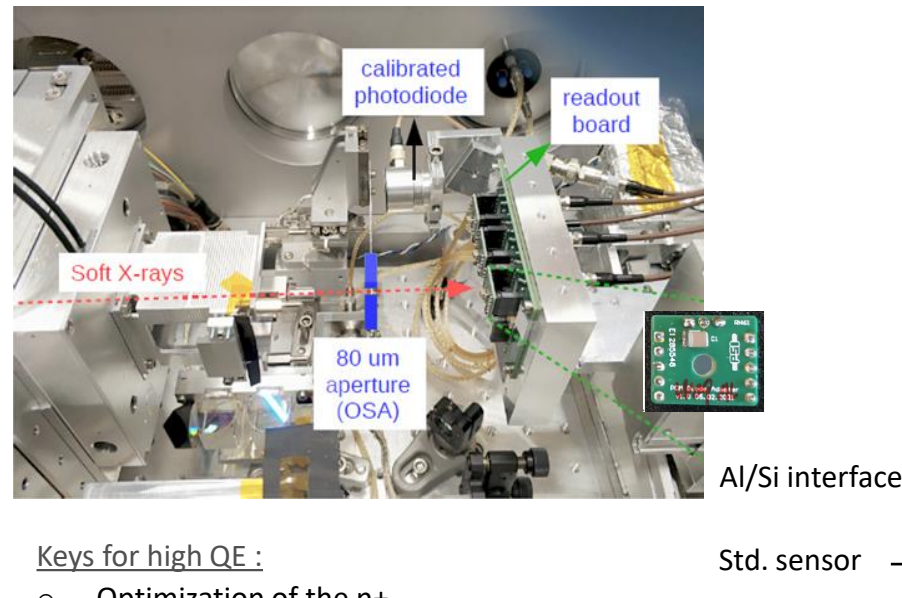
Std. sensor

## Quantum efficiency

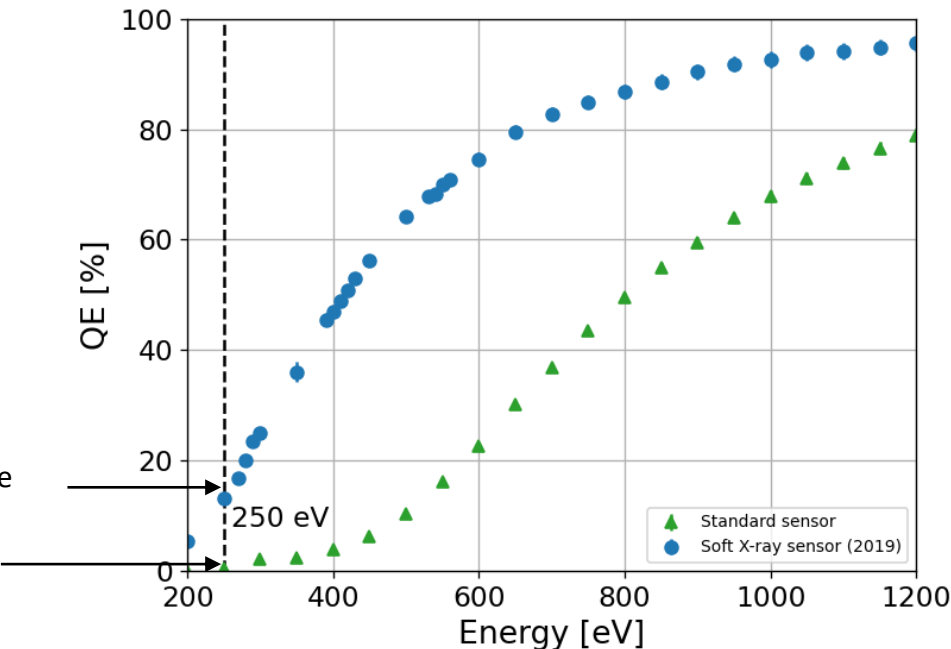


# QE improvement

## Setup at the Surface/Interfaces Microscopy (SLS)

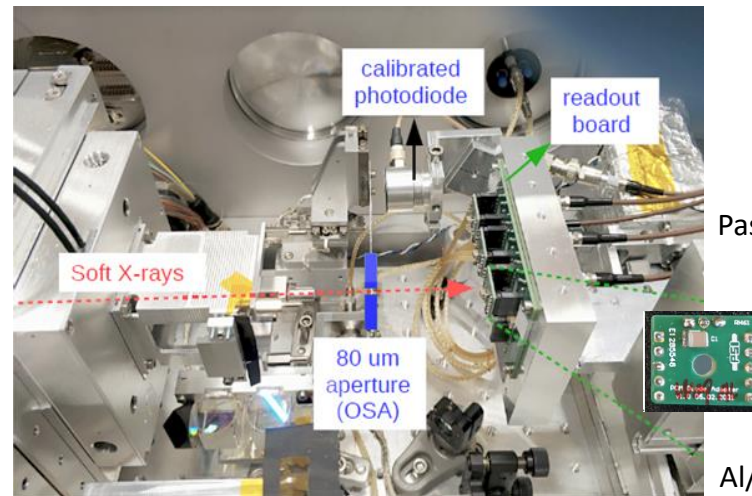


## Quantum efficiency



# QE improvement

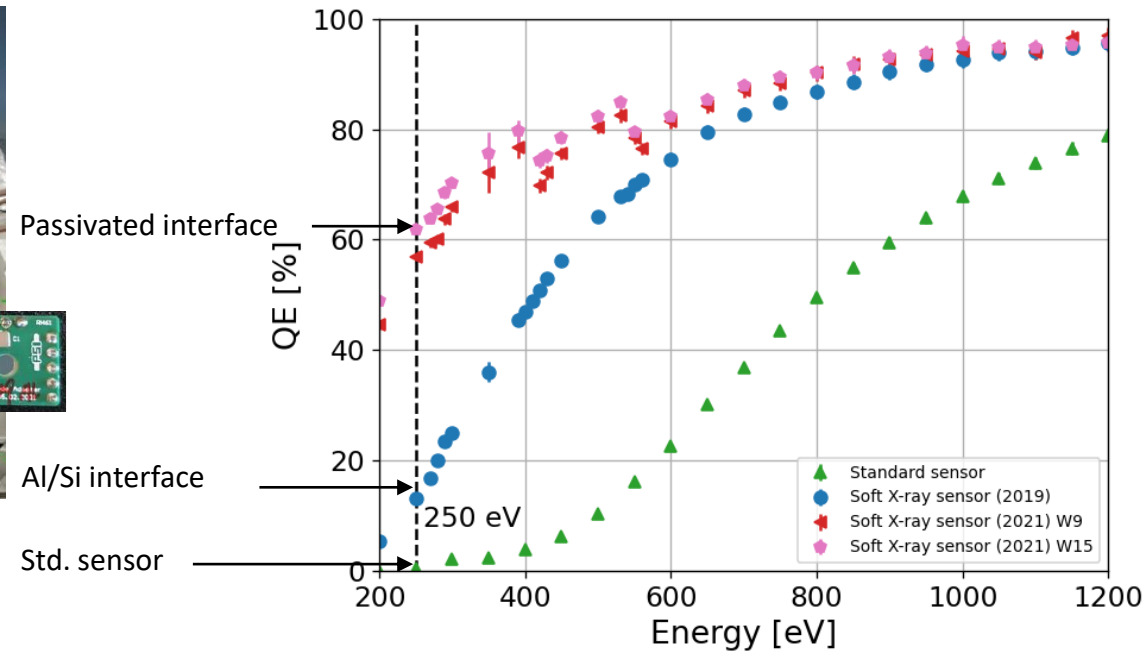
## Setup at the Surface/Interfaces Microscopy (SLS)



### Keys for high QE :

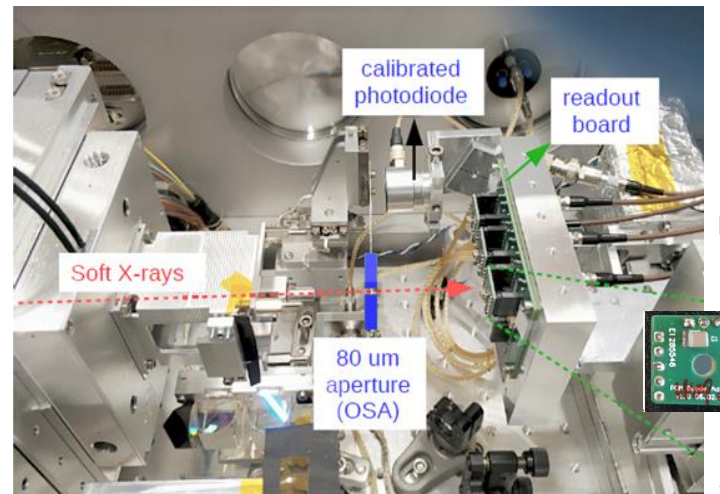
- Optimization of the n+
- Surface passivation

## Quantum efficiency



# QE improvement

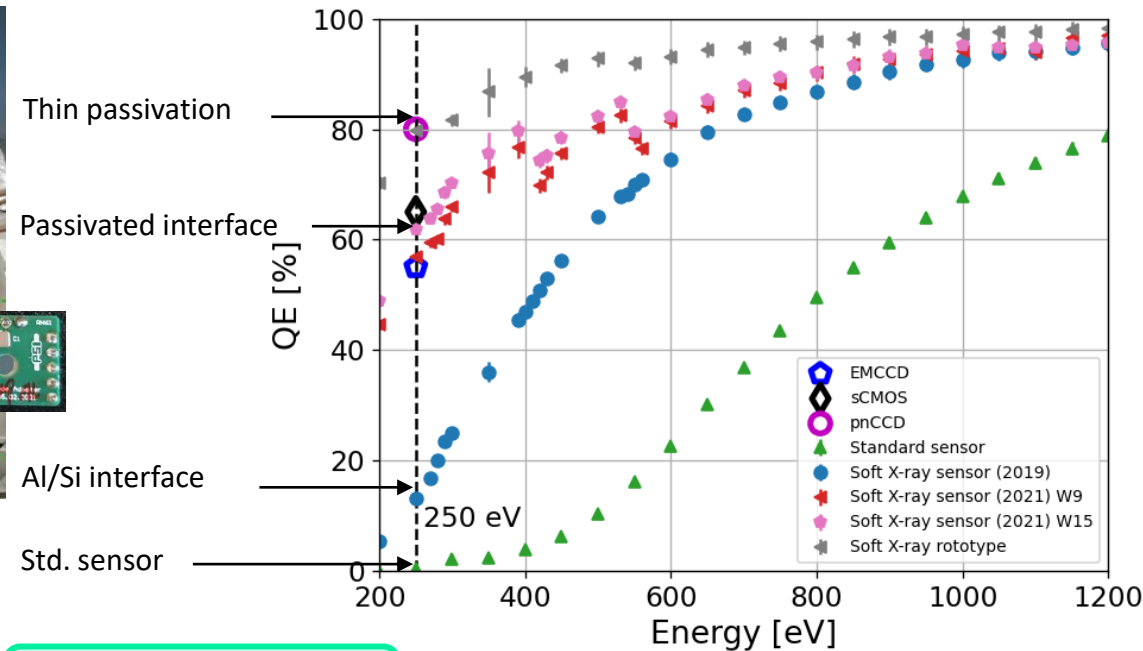
## Setup at the Surface/Interfaces Microscopy (SLS)



### Keys for high QE :

- Optimization of the n+
- Surface passivation
- Reduction of the passivation layer

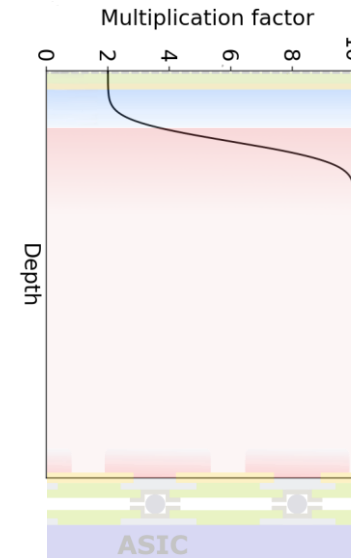
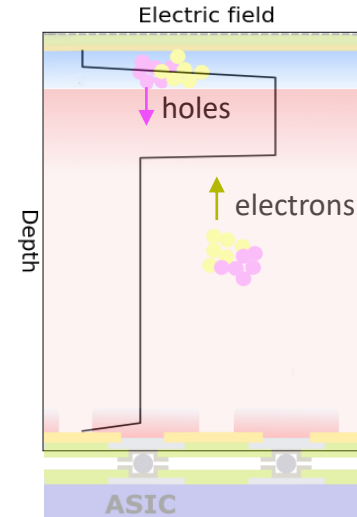
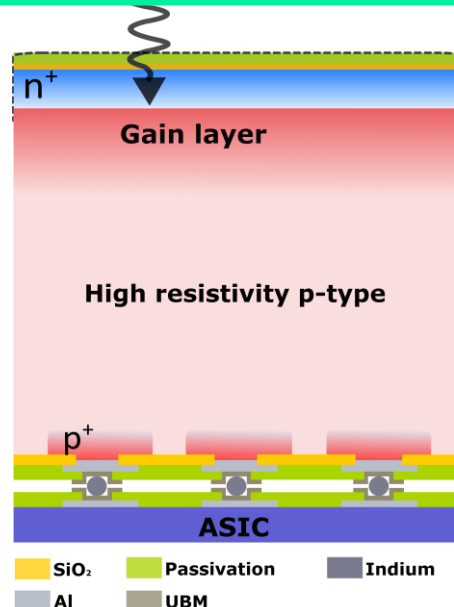
## Quantum efficiency



# iLGADs for soft X-ray detection

## Inverse low-gain avalanche diode (iLGAD) technology

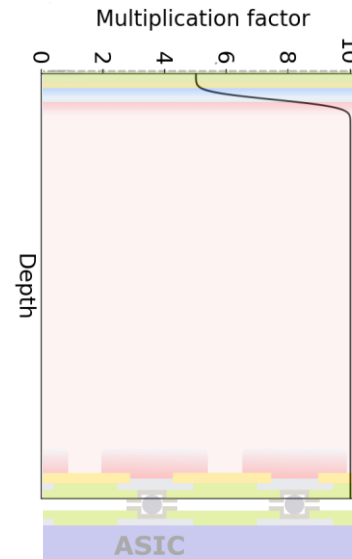
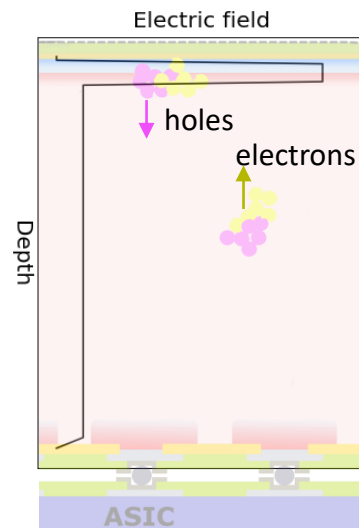
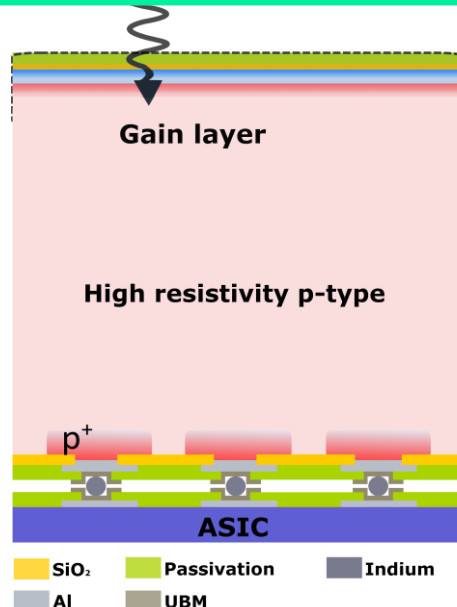
- Large electric field triggers impact ionization
- Gain depends on absorption depth



# iLGADs for soft X-ray detection

## Inverse low-gain avalanche diode (iLGAD) technology

- Large electric field triggers impact ionization
- Gain depends on absorption depth
- Move gain layer to the surface



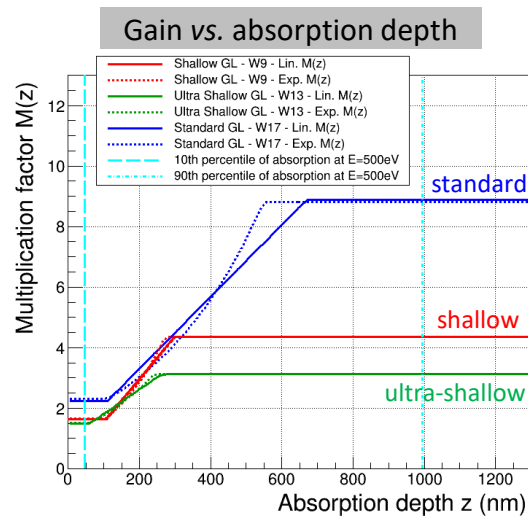
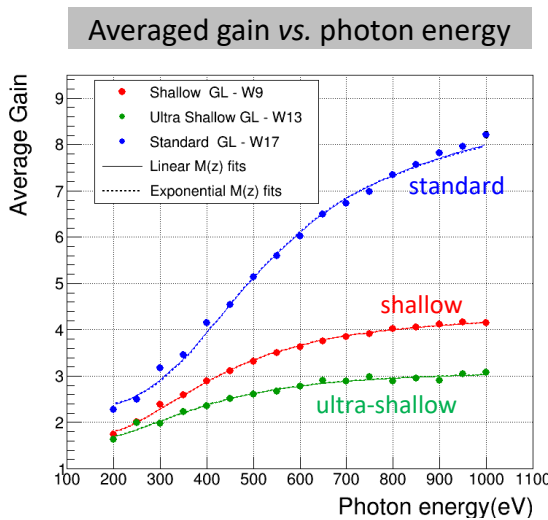
# Depth dependence of gain in iLGADs

QE value equal to the TEW batch

- ~ 60 % for 250 eV photons

Averaged gain measured for different gain-layer designs

- standard, shallow and ultra-shallow gain-layer designs



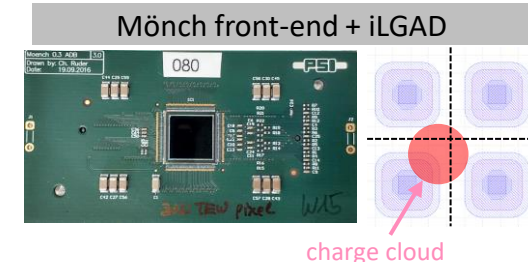
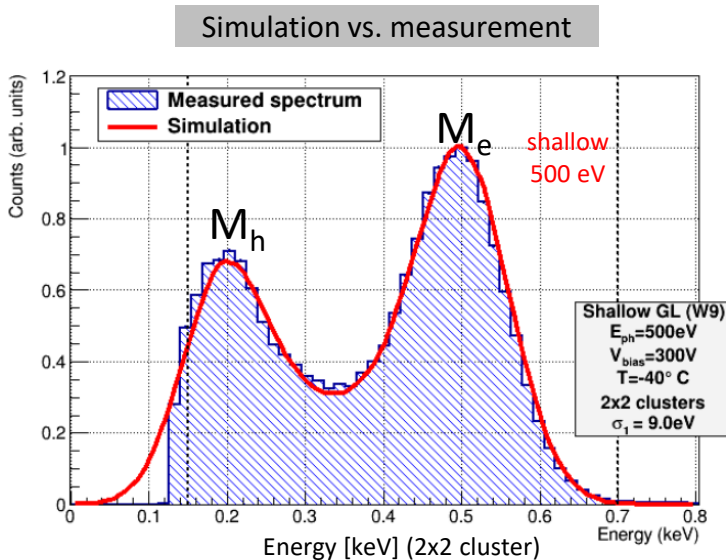
Shallow

- Gain-layer ~ 300 nm
- Smaller ratio between Me/Mh
- Low Me gain due to an overestimation of the impact ionization coefficients

# Depth dependence of gain in iLGADs

## Monte-Carlo simulation of charge drift, diffusion and multiplication

- Mönch (25 μm pitch) with Shallow gain-layer design
- Photon energy 500 eV
- Cluster 2x2



- Two peaks  $M_e$  and  $M_h$
- $M_e$  X-ray is absorbed after the gain layer ( $G \uparrow$ )
- $M_h$  X-ray is absorbed before the gain layer ( $G \downarrow$ )

Antonio Liguori et al 2023 JINST 18 P12006  
<https://doi.org/10.1088/1748-0221/18/12/P12006>

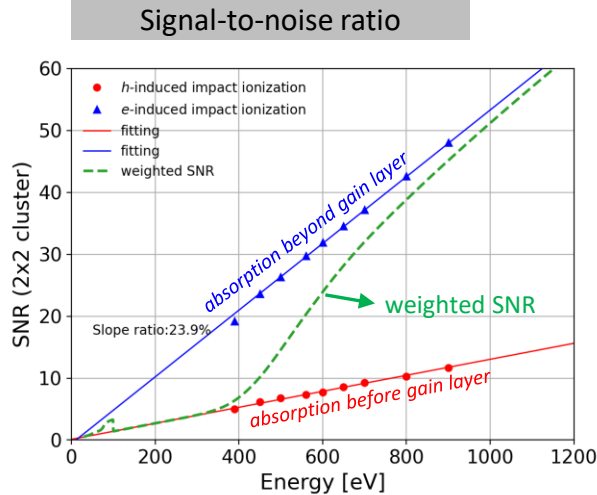
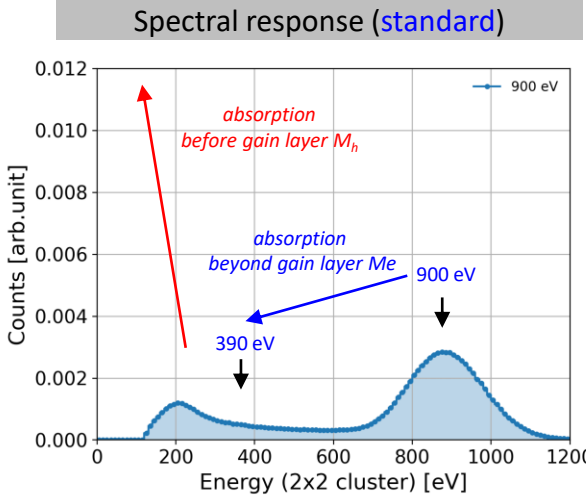
# Single photon resolution



## iLGAD measurement @ SIM (SLS):

- Photon energies: 390 eV to 900 eV
- Standard gain-layer design
- Temperature ↓ → Leakage current ↓ Gain ↑
- Photon energy ↓ →  $M_e$  counts ↓  $M_h$  counts ↑

V. Hinger et al, Front. Phys., 28 February 2024  
Sec. Radiation Detectors and Imaging  
Volume 12 - 2024 | <https://doi.org/10.3389/fphy.2024.1352134>



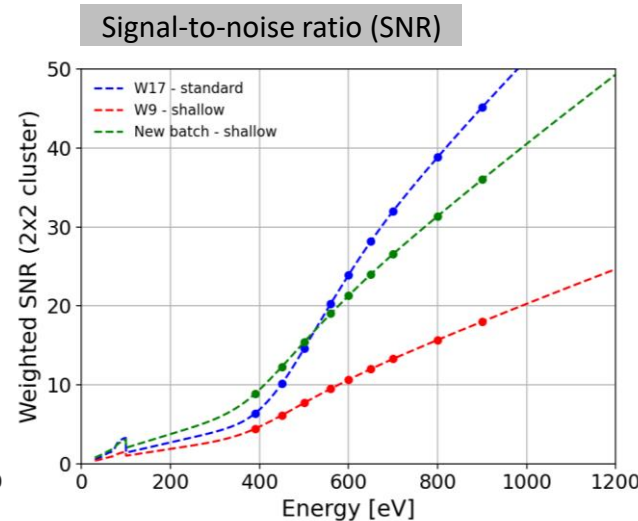
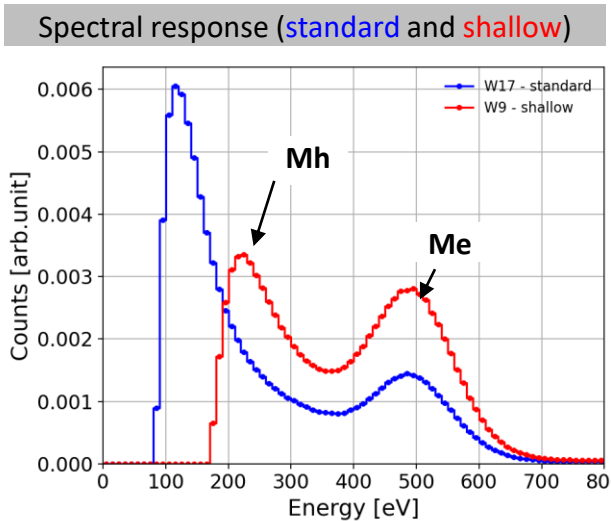
- Single photon resolution ( $E > 390$  eV)
- Two peaks ( $M_e$  and  $M_h$ )
- Weighted SNR  $\rightarrow$   $SNR_h$  ( $E < 500$  eV)
- Requires 2x gain @ 250 eV

# Comparison between gain layers



## iLGAD measurement @ SIM (SLS):

- Standard and shallow gain-layer designs (500 eV)
- Shallow design shows large # of count for  $M_e$
- Weighted SNR (shallow), gain needs to be increased by a factor of 2 (like standard)



- Higher # counts in  $M_e$  (shallow)
- Similar effective SNR ( $E < 350$ eV)
- Next R&D Shallow design with x2 gain

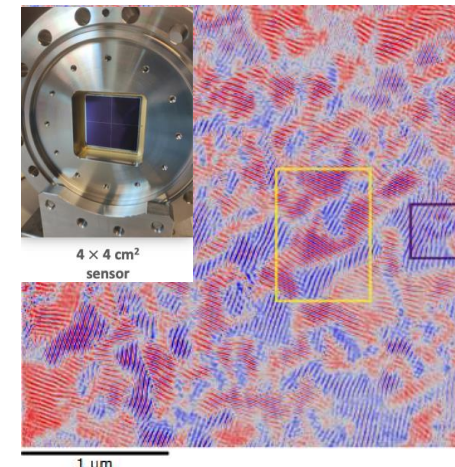
# Summary and Outlook

## TEW development:

- Important: reduction of concentration and depth of n+, passivation of the surface and thinning of the passivation
- QE was improved from 1% up to 62% (80% prototype) for 250 eV photons
- A new batch with further optimisation of the passivation is expected in October
- Systematic study of the QE after irradiation

## iLGAD development for soft X-rays:

- The spectral response shows two peaks
- Single photon resolution down to 390 eV for standard and shallow design of the gain layer
- Shallow design shows a higher probability of photon absorbed after the gain layer
- First user experience of Eiger+iLGAD to study BiFeO<sub>3</sub> thin film. Spin cycloids ->64 nm period.
- Study of the gain suppression effect. Jiaguo's poster in Session 2 (ID: 141) July 3, 14:00 - 15:10
- Study of the iLGAD response at high intensities.
- Next iLGAD batch, SPC and CI + iLGAD detectors with single photon resolution (E>250 eV)



T. A. Butcher, et al. Ptychographic Nanoscale Imaging of the Magnetoelectric Coupling in Freestanding BiFeO<sub>3</sub>.  
Adv. Mater. 2024, 2311157. <https://doi.org/10.1002/adma.202311157>

# Acknowledgement

## My thanks go to:

- Colleagues from FBK
- K.Vogelsang and C.Wild from LBNL
- A. Kleibert, J. Raabe, S. Finizio and T. Butcher from the SLS.
- A. Liguori from University Bari
- Two of the authors (V. Hinger and K. A. Paton) have received funding from MSCA PSI-FELLOW-III-3i (EU grant agreement No. 884104)

## Postdoc positions open:

LGAD



ASIC



## Photon Science Detector Group

*Back from left to right: B. Braham, K. Moustakas, C. Ruder, D. Greiffenberg, J. Heymes, K. Ferjaoui, C. Lopez-Cuenca, K. Kozlowski, M. Brückner, K. A. Paton, F. Baruffaldi, T. King, and P. Sieberer. Front: J. Zhang, V. Hinger, S. Hasanaj, A. Bergamaschi, X. Xie, R. Dinapoli, and B. Schmitt. Missing: R. Barten, S. Ebner, E. Fröjd, D. Mezza, A. Mozzanica and D. Thattil.*

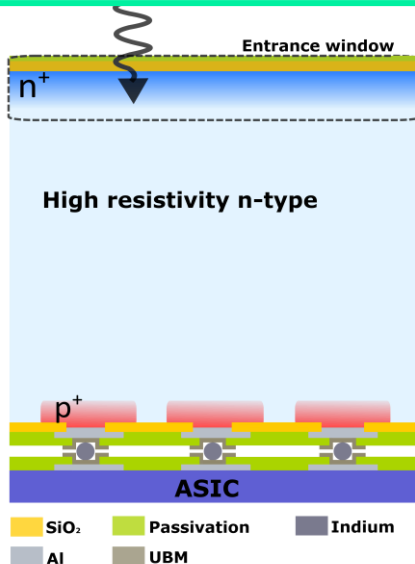


# Backup

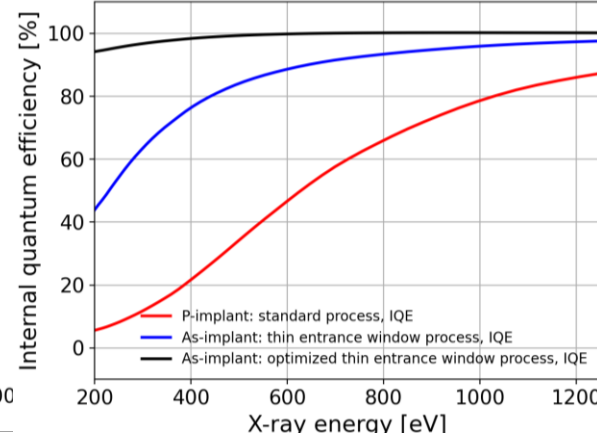
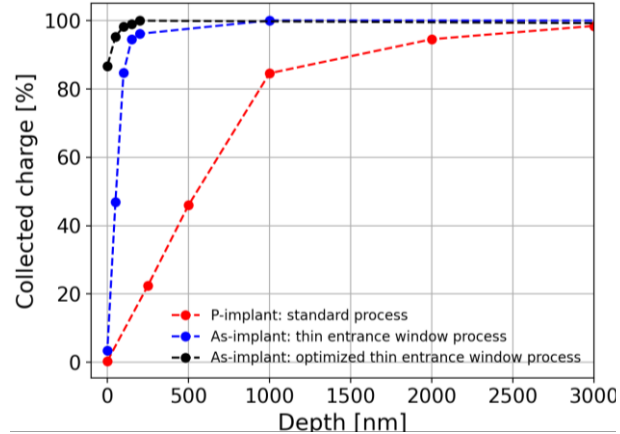
# Development strategy

## Thin entrance window technology

- Optimization of the n+
- Passivation of the surface



## TCAD simulation of the process and device

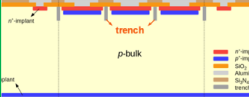


Internal QE larger than 90 %

J. Zhang *et al* 2022 JINST 17 C11011

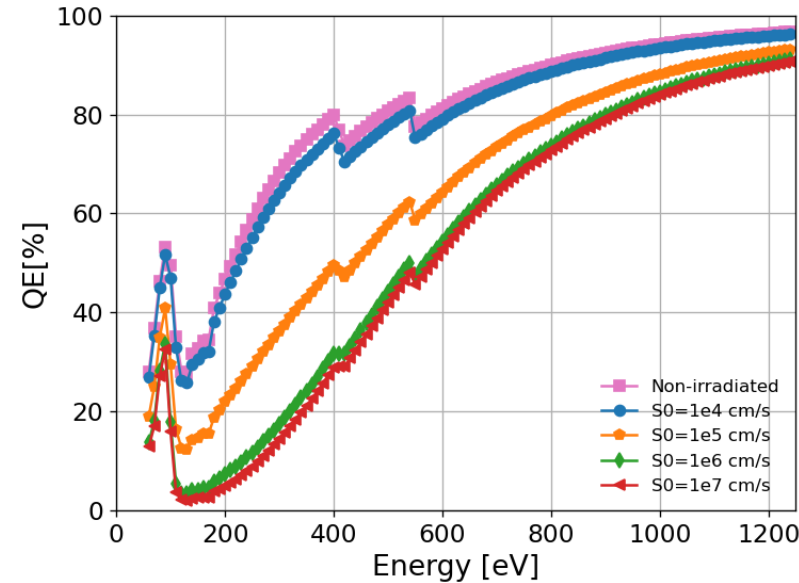
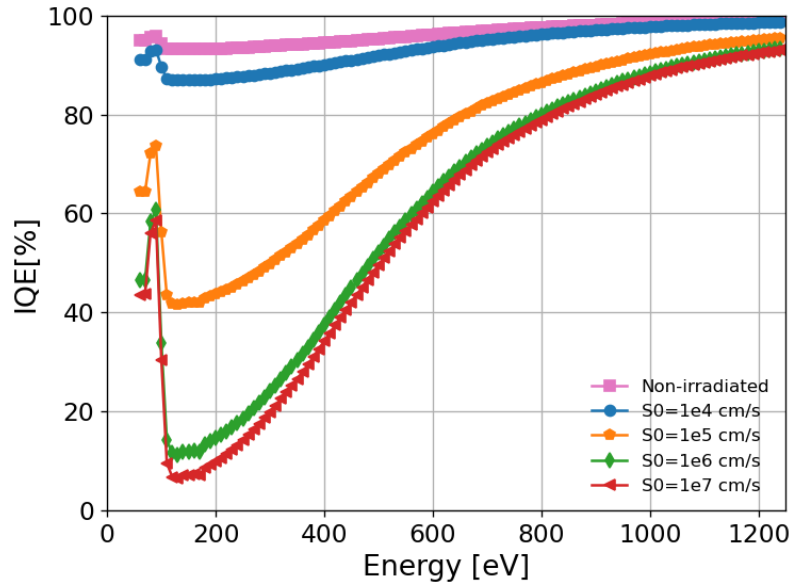
<https://doi.org/10.1088/1748-0221/17/11/C11011>

# LGAD technologies

	LGAD	inverse-LGAD (iLGAD)	trench-isolated LGAD (TI-LGAD)	AC-coupled LGAD (AC-LGAD)	deep junction LGAD (DJ-LGAD)	ideal LGAD
cross section	 <p>n<sup>+</sup> implant p-bulk JTE</p> <p>Legend: n<sup>+</sup> implant, p<sup>+</sup> implant, p-bulk, SiO<sub>2</sub>, Aluminum, Si<sub>3</sub>N<sub>4</sub></p>	 <p>p<sup>+</sup> implant p-bulk n<sup>+</sup> implant p<sup>+</sup> implant n<sup>+</sup> implant p<sup>+</sup> implant p-bulk trench</p> <p>Legend: n<sup>+</sup> implant, p<sup>+</sup> implant, p-bulk, SiO<sub>2</sub>, Aluminum, Si<sub>3</sub>N<sub>4</sub></p>	 <p>n<sup>+</sup> implant trench p-bulk n<sup>+</sup> implant p-bulk</p> <p>Legend: n<sup>+</sup> implant, p<sup>+</sup> implant, p-bulk, SiO<sub>2</sub>, Aluminum, Si<sub>3</sub>N<sub>4</sub></p>	 <p>n<sup>+</sup> implant capacitive coupled to the readout p-bulk n<sup>+</sup> implant p-bulk</p> <p>Legend: n<sup>+</sup> implant, p<sup>+</sup> implant, p-bulk, SiO<sub>2</sub>, Aluminum, Si<sub>3</sub>N<sub>4</sub></p>	 <p>n<sup>+</sup> implant deep-junction (gain) layer p-bulk n<sup>+</sup> implant p-bulk</p> <p>Legend: n<sup>+</sup> implant, p<sup>+</sup> implant, p-bulk, SiO<sub>2</sub>, Aluminum, Si<sub>3</sub>N<sub>4</sub></p>	?
process*	standard	double-sided	stepper	standard	epi-growth	standard
complexity	low	low	medium	high	high	low
collected charge	e <sup>-</sup>	h <sup>+</sup>	e <sup>-</sup>	e <sup>-</sup> (bipolar)	e <sup>-</sup>	e <sup>-</sup> or h <sup>-</sup>
readout	DC	DC	DC	AC	DC	DC
non-gain region (fill factor)	> 40 um low	0 um 100%	6-7 um high	0 um 100%	0 um 100%	0 um 100%
gain depends on absorption depth	no	yes	no	no	no	no
detection area	large	medium-large	small	medium-large	medium-large	large
multiplication of surface current	no	yes	no	yes	yes	no
risk/yield	low/good	medium/medium	medium/medium	medium/medium	high/low	low/good

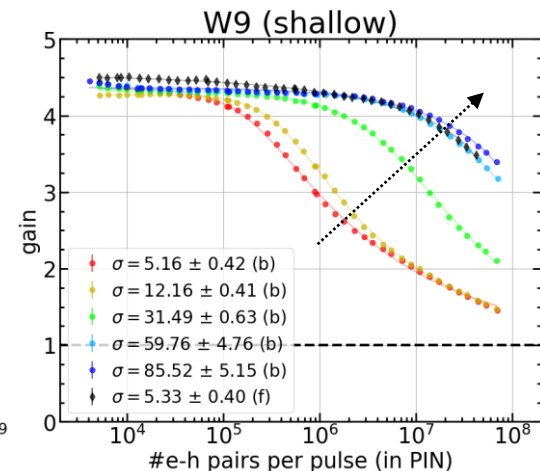
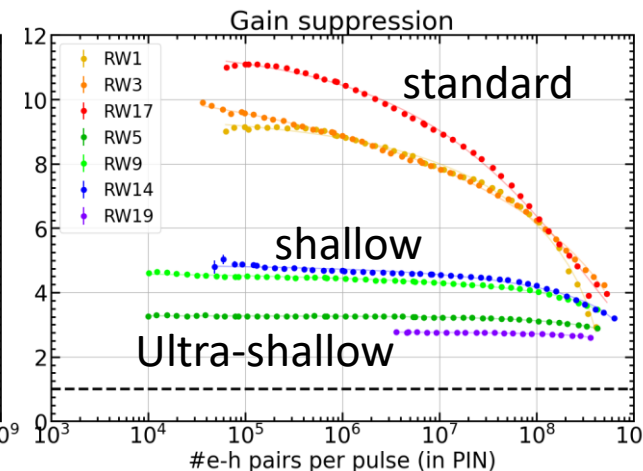
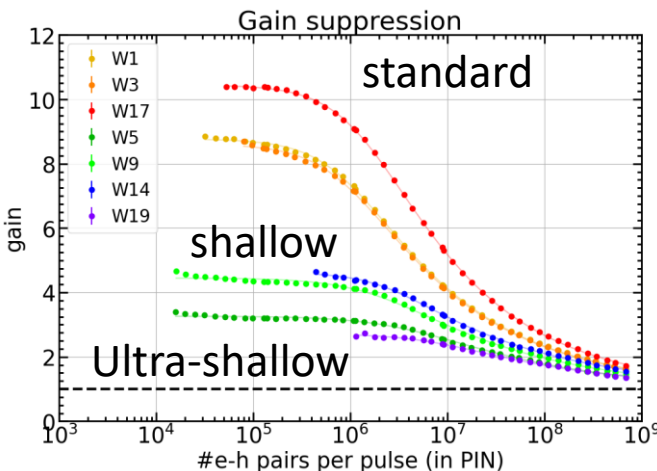
# IQE and QE after irradiation

$S_0$  saturates to  $1e4$  cm/s



# Gain suppression

- Red laser (660 nm), repetition rate (5 MHz), Beam  $\sigma \sim 4 \mu\text{m}$
- Observed gain suppression for front(gain layer) and back (pixel) side illumination
- Gain suppression depends on :
  - Beam intensity and size (# e-h pairs per pulse and density)
  - Charge-carrier density at the gain layer
  - Gain layer design and multiplication factor

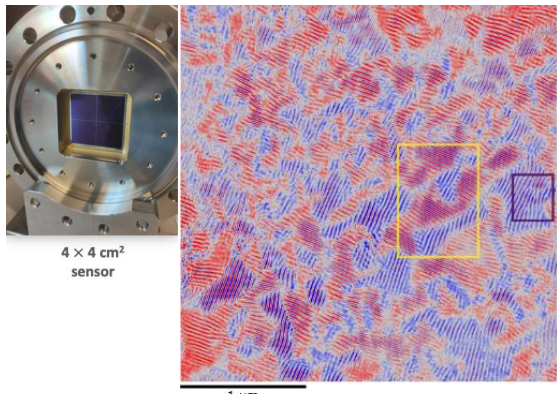


# Photon science with iLGADs

## EIGER (single-photon counting) + iLGADS @ SIM-SLS

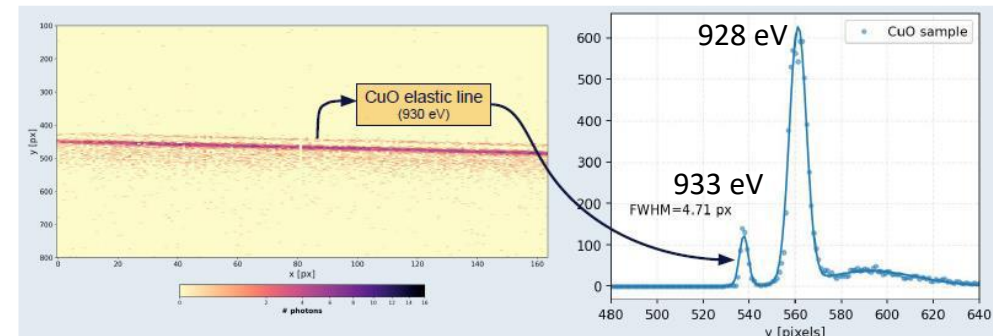
- EIGER+ iLGAD for ptychography (User friendly 😊)
- Dichroic contrast at Fe L<sub>3</sub> edge (712.5 eV) of BiFeO<sub>3</sub> thin film
- Improved resolution down to 6 nm (vs. 15 nm with Mönch + standard sensor)

### Ptychography EIGER + iLGAD



## JUNGFRAU(charge integrating) + strixel iLGADS @ EuXFEL

- JUNGFRAU+ iLGAD for RIXS



First user experiment using an iLGAD sensor where spin cycloids with 64 nm period were observed

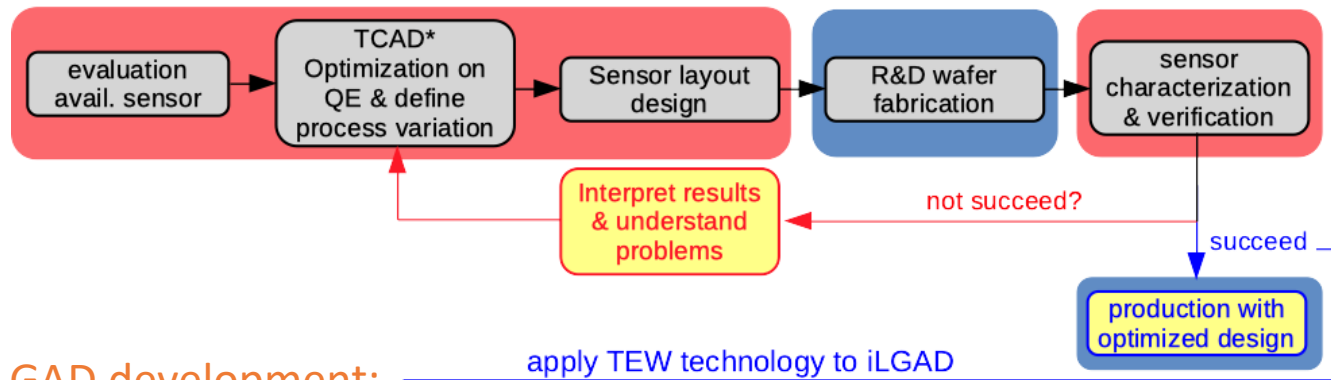
T. A. Butcher, et al. Ptychographic Nanoscale Imaging of the Magnetoelectric Coupling in Freestanding BiFeO<sub>3</sub>.  
Adv. Mater. 2024, 2311157. <https://doi.org/10.1002/adma.202311157>

# Development strategy

Two developments for hybrid detectors towards soft X-rays:

- Thin entrance window (TEW) process
- iLGADs optimised for soft X-rays

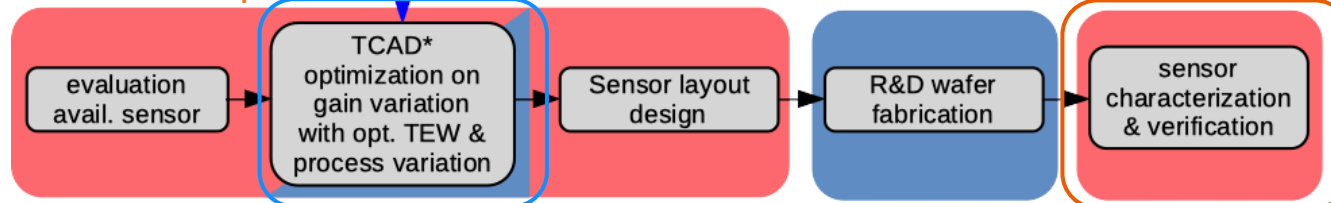
## TEW development:



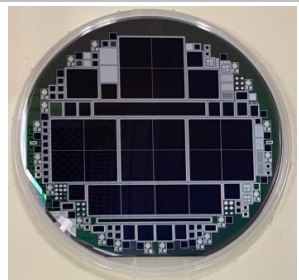
6-inch TEW wafers 2021



## iLGAD development:



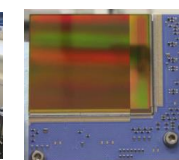
6-inch iLGAD wafers 2022



## commercial

## Facility / institute driven development

Parameter	Andor iXon Ultra 888 (EMCCD)	Andor Neo 5.5 sCMOS	Princeton Instruments PIXIS 1024BR (CCD)	Hamamatsu ORCA-Fusion (CMOS)	pnCCD (PNSENSOR)	DSSC (EuXFEL)	PERCIVAL (DESY)	Hybrid X-ray detector (PSI, Jungfrau)
Quantum Efficiency (QE) @250 eV	55% (400 nm UV)	70% (400 nm UV)	< 42% (400 nm UV)	65% (400 nm UV)	80%	52%	90%	80%
Read Noise (e-)	< 1	1.4	4-10	1.4	10.5 (hg)	40-60 (miniSDD) 10 (DEPFET)	16	3 - 5 (LGAD)
Frame Rate (FPS)	26	30 (full frame) 100 (burst)	< 2	< 100	< 100	4.5 MHz (burst)	< 120	2 - 10 k
Dynamic Range (e-)	80 k	30 k	100 k	15 k	1.6 M	1.1 M	3.5 M	3.44 M (gain=10)
Pixel Size ( $\mu\text{m}$ )	13 x 13	6.5 x 6.5	13 x 13	6.5 x 6.5	75 x 75	204 x 236	27 x 27	75 x 75 15 x 375
Pixels	1024 x 1024	2560 x 2160	1024 x 1024	2304 x 2048	512 x 1024	128 x 256	1484 x 1408	512 x 1024
Sensor Area ( $\text{mm}^2$ )	13.3 x 13.3	16.6 x 14.0	13.3 x 13.3	14.9 x 13.3	38.4 x 76.8 (2 side buttable)	30 x 62 (tiable)	40 x 38	38.4 x 76.8 (tilable)



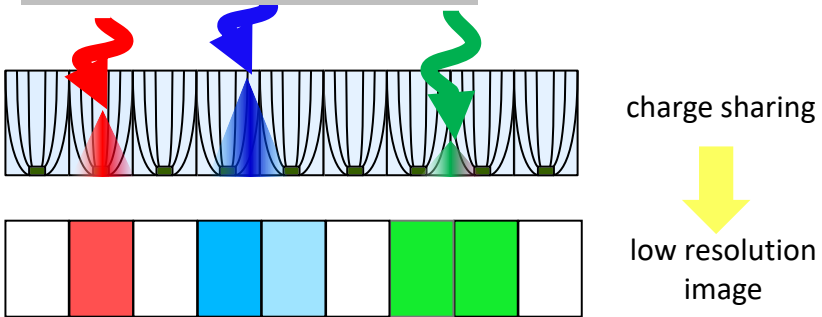
# Interpolation with iLGADs



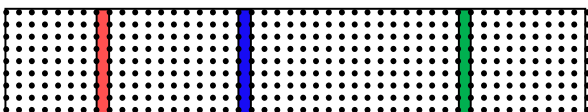
# Soft X-ray interpolation @ POLLUX (SLS)

- 25 um pitch Mönch + iLGAD sensor (**shallow**)
  - Demonstrates Charge sharing and interpolation at 500eV

**1**

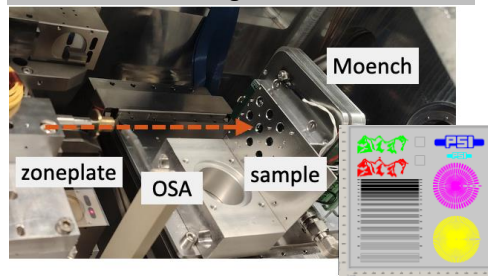


$$\eta = \frac{Q_{right}}{Q_{right} + Q_{left}}; \color{red}{\eta = 1}; \color{blue}{\eta = 0.25}; \color{green}{\eta = 0.5};$$

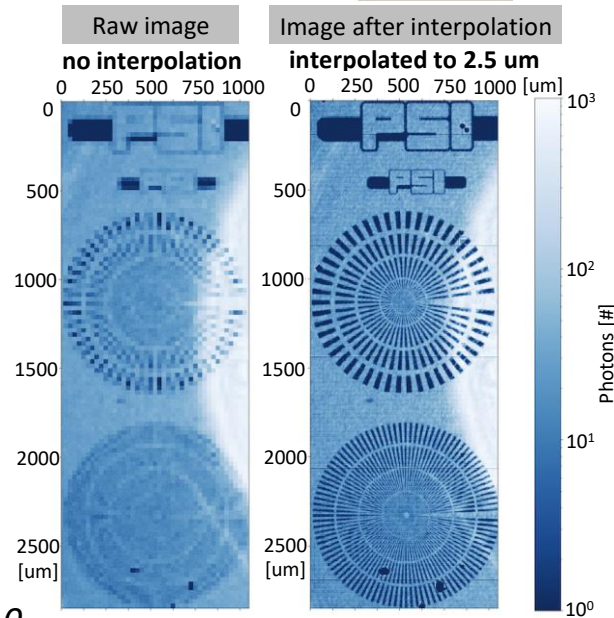


high resolution  
image

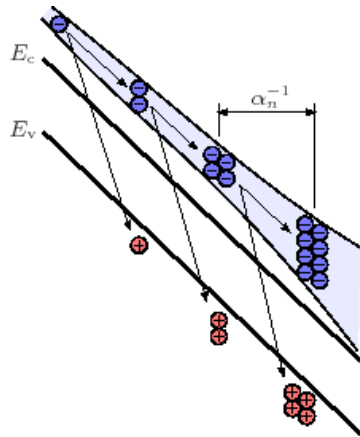
### Transmission image unfocused beam



Sample prepared  
by X-ray  
Optics group



# Impact ionization



Massey:

$$\alpha_{n,p}(E, T) = A_{n,p} \exp\left(-\frac{C_{n,p} + D_{n,p}T}{E}\right)$$

Van Overstraeten:

$$\alpha_{n,p}(E, T) = \gamma A_{n,p} \exp\left(-\gamma \frac{B_{n,p}}{E}\right)$$

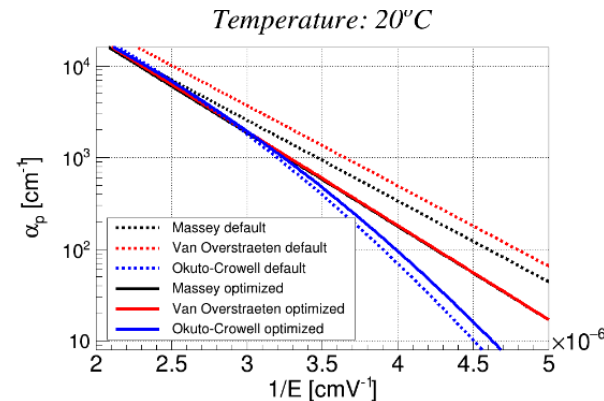
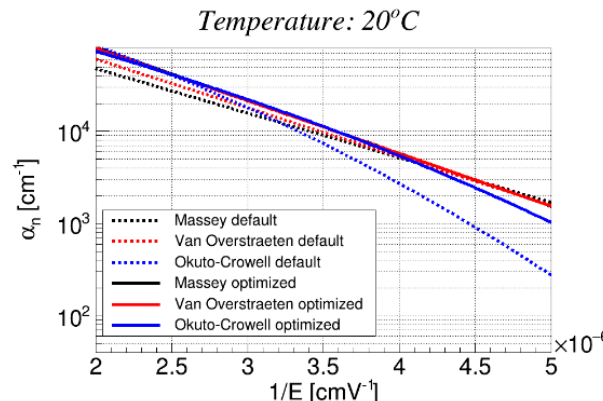
$$\gamma = \frac{\tanh \frac{\hbar \omega_{op}}{2kT_0}}{\tanh \frac{\hbar \omega_{op}}{2kT}}$$

Okuto-Crowell:

$$\alpha_{n,p}(E, T) = A_{n,p} (1 + (T - 300) C_{n,p}) E \times \exp\left[-\left(\frac{B_{n,p} (1 + (T - 300) D_{n,p})}{E}\right)^2\right]$$

Pure electron started impact ionization

O. Triebel, "Reliability Issues in High-Voltage Semiconductor Devices"



Currás Rivera and Moll (*IEEE Trans. Electron Devices* 2023 **70** 2919–2926)

<https://ieeexplore.ieee.org/stamp/stamp.jsp?arnumber=10114953>